

F. Vannini¹, A. Biancalani¹, A. Bottino¹,
T. Hayward-Schneider¹, Ph. Lauber¹, A. Mishchenko², I. Novikau¹, E. Poli¹ and the ASDEX Upgrade Team

¹Max-Planck-Institut für Plasmaphysik, 85748 Garching, Germany
²Max-Planck-Institut für Plasmaphysik, 17491 Greifswald, Germany

1. Introduction and Motivations

- **Shear Alfvén eigenmodes** [1] are instabilities interacting with energetic particles (EPs) in tokamak plasmas [1, 2]. They can lead to EP redistribution and losses.
- Alfvén eigenmodes are observed in ASDEX Upgrade [3].
- The electromagnetic, global, gyrokinetic PIC code **ORB5** [4, 5, 6] is used here, with the new pull-back scheme. Its model contains reduced MHD as subset. It includes additionally finite-Larmor radius and finite-orbit-width effects and Landau damping on all species.

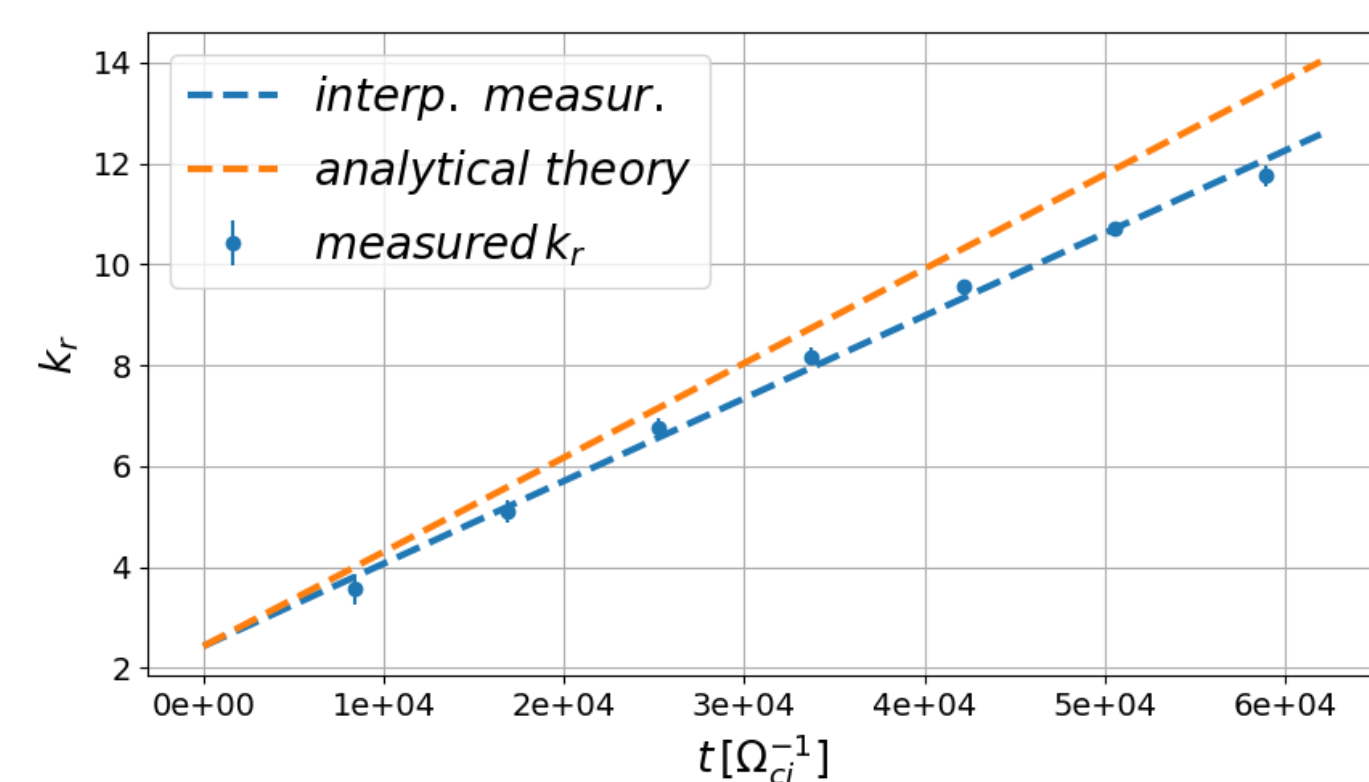
2. Continuum Damping

- Cylinder limit ($\epsilon = a_0/R_0 = 0.01$), flat density and temperature profiles ($n_e = n_i = 2.22 \cdot 10^{20} m^{-3}$, $T_e = T_i = 0.01 KeV$).
- Because of the low temperatures in use and of the finite value of the shear, we expect the **Continuum Damping** to be the main damping mechanism in this case [7].
- Safety factor profile: $q(s) = q_0 + q_1 s$, where $s = \sqrt{\psi/\psi_{edge}}$ and ψ is the poloidal magnetic flux.
- Initial perturbation: axisymmetric electrostatic potential (ϕ) with $n = 0$, $m = 1$, peaked at $s = 0.6$.
- For the case under investigation $\Omega_{ci} = q_i B_0/(m_i c) = 2.87 \cdot 10^8 rad/s$. Alfvén speed is constant and equal to $v_A = 4.38 \cdot 10^5 m/s$.

$$\delta\phi \sim \frac{1}{k_r(t)} \quad k_r(t) = k_{r,0} + k_{r,1}t \quad (1)$$

$$k_{r,1} = -\frac{\partial\omega(s)}{\partial s} \quad \omega = \frac{v_A}{q(s)R_0}$$

- A new diagnostic for the measurement of k_r has been developed. Results show a linear dependence in k_r in agreement with the theoretical expectations, [8].



- The potentials decay according to Eq.1, Figure 1: Measure of the radial wavenumber k_r as a function of time. The shown results correspond to a simulation with $q_1 = 0.5$ and q_0 set in order to have $q(s_0) = 2$.

3. Electron Landau Damping

- Inverse aspect ratio: $\epsilon = 0.1$. Flat temperature profiles. $\Omega_{ci}/\omega_{A0} \sim 196$.
- When considered, the energetic particles (**EP**) have an on-axis density profile.
- The magnetic equilibrium and profiles are those of the ITPA-TAE international benchmark case [9].
- Initial perturbation: electrostatic potential with $n = 6$ and $9 \leq m \leq 12$. A Toroidal Alfvén Eigenmode (**TAE**) is observed at $s = 0.5$, given by the interaction of the two close modes $m = 10$, $m = 11$.
- For the considered bulk plasma temperatures, we expect the Landau damping to be the main damping mechanism and the continuum damping to be negligible.
- An analytical estimation of the Landau damping has been given, following [10, 11, 12]. According to this, the contribution given by the bulk ions appears to be negligible as compared to that of the bulk electrons.

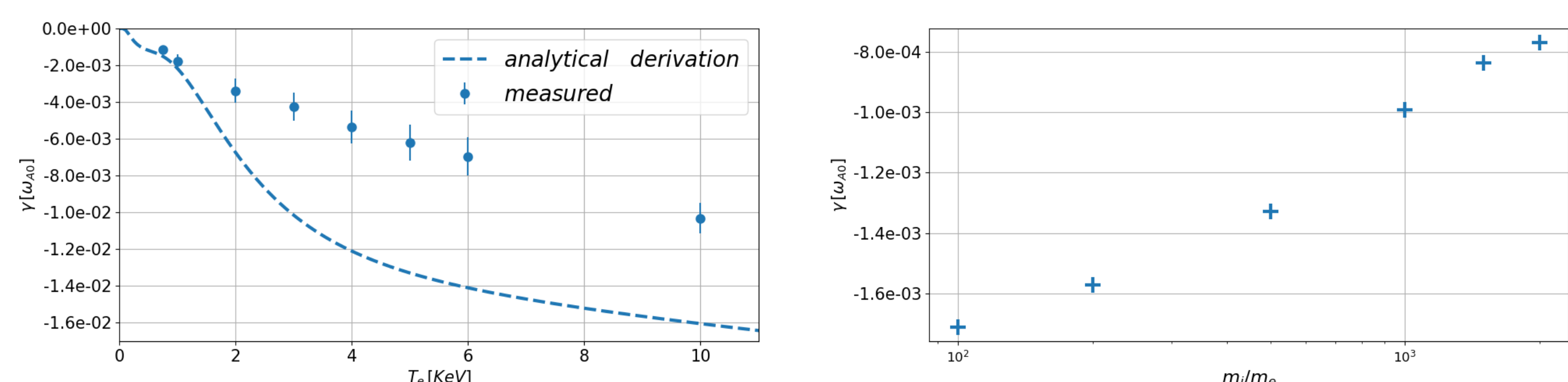


Figure 2: **Left:** Landau damping dependence versus the electron temperature ($m_e/m_e = 200$). This is a proof that the dominant damping is indeed the electron Landau damping. **Right:** Damping rate dependence on the electron mass.

- A reasonable agreement between the analytical theory and the damping rate for this case has been found, confirming that for the present case the Landau damping is dominant over the Continuum damping.

4.0 NLED-AUG case: # 31213 @ 0.84s

- The magnetic equilibrium from the experimental case of **ASDEX-Upgrade** shot number 31213 @0.84s are considered. Details can be found in [3].

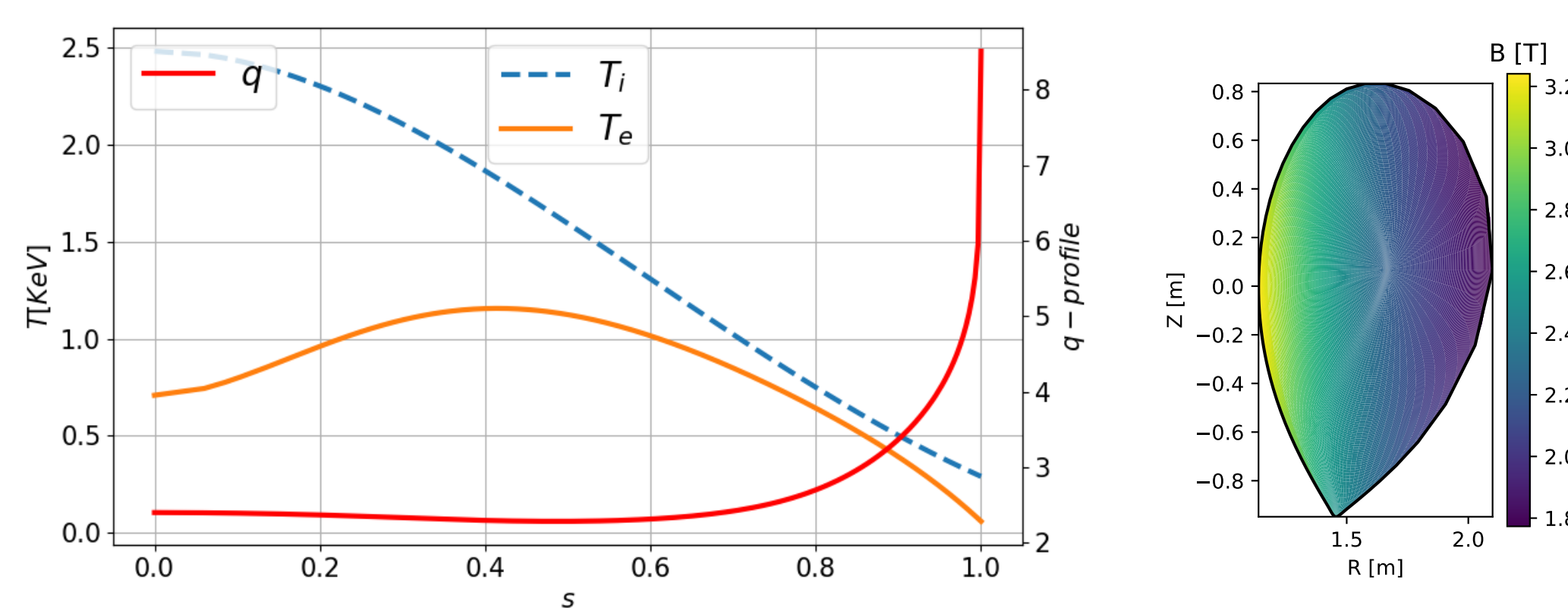


Figure 3: Profiles and magnetic equilibrium.

Reference

- [1] L. Chen and F. Zonca *Rev. Mod. Phys.* **88**, 015008 (2016)
[2] K. Appert et al., *Plasma Phys* **24**, 1147 (1982)
[3] Ph. Lauber, http://www2.ipp.mpg.de/~pw1/NLED_AUG/data.html
[4] S. Jolliet et al., *Comput. Phys. Comm.* **177**, 409 (2007)
[5] A. Bottino et al. *Plasma Phys. Control. Fusion* **53**, 124027 (2011)
[6] Mishchenko A. et al., *Comput. Phys. Comm.* **238**, 194-202 (2019)
[7] L. Chen and A. Hasegawa, *Physics of Fluids* **17**, 1399 (1974)
[8] G. Vlad et al., *Rivista del Nuovo Cimento* **22**, 7 (1999)
[9] A. Köniies et al., *Nuclear Fusion* **58**, 126027 (2018)
[10] L. Chen, *Editrice Compositori, Bologna* **17**, (1989)
[11] Kolesnichenko Ya.I. et al., *Nucl. Fusion* **56**, 066004 (2016)
[12] Betti R. and Freidberg J.P., *Physics of Fluids B* **4**, 1465 (1992)
[13] P. Lauber et al., *Phys. Plasmas* **12**, 122501 (2005)
[14] G. Fogaccia, G. Vlad, S. Briguglio, *Nucl. Fusion* **56**, 112004 (2016)
[15] Novikau I. et al., *AAPPS-DPP*, (2019) (to be presented)

Acknowledgments

Simulations were performed on the CINECA Marconi supercomputer within the ORBFAST project. The author would like to thank the ORB5 team, Xin Wang and Zhixin Lu for useful discussions. This work was partly performed in the frame of the “Multi-scale Energetic particle Transport in fusion devices” ER project.

4.1 NLED-AUG case: linear results

- In simulations involving EPs, both on-axis and off-axis density profiles have been considered. EPs have a flat temperature profile.
- Initial perturbation: ϕ with $n = 1$ and $0 \leq m \leq 6$. The dominant poloidal modes are $m = 2, 3$.
- Simulations have been performed with and without finite Larmor radius (FLR) effects.

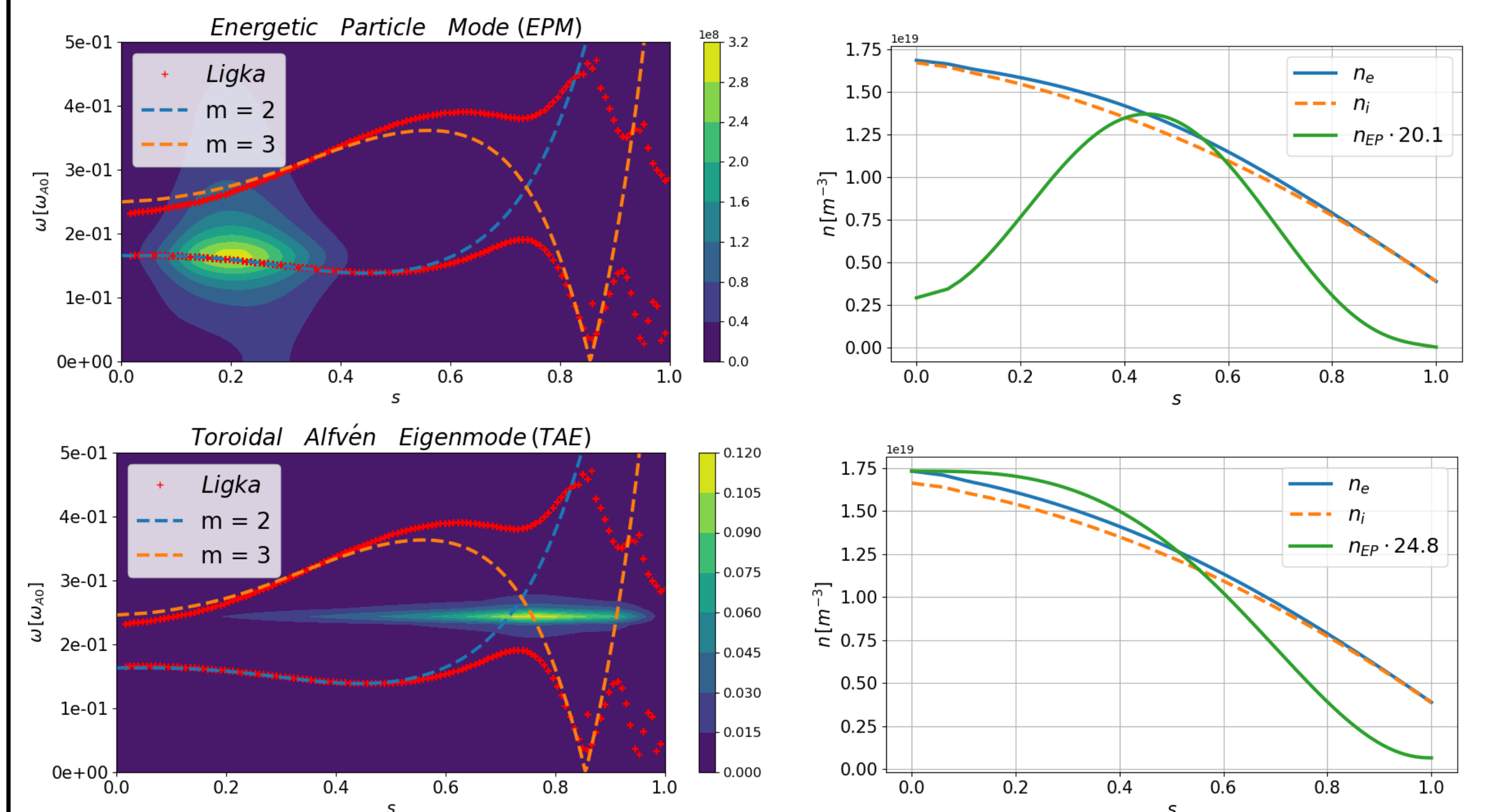


Figure 4: Frequency spectra (**Left**), obtained for different EPs's profiles (**Right**). The continuous frequency spectra calculated with the code LIGKA [13] (red crosses) and with the use of the MHD-theory (dotted lines) are also shown. In these simulations ions and EPs FLR-effects are neglected.

- Experimental spectrogram obtained with Mirnov coils [3]. At $t = 0.84 s$ is shown the simulation result obtained with ORB5.
- The result from the simulation is obtained neglecting FLR effects.
- When FLR effects are included we observe only a slight change in the frequency from 129 to 131 KHz.

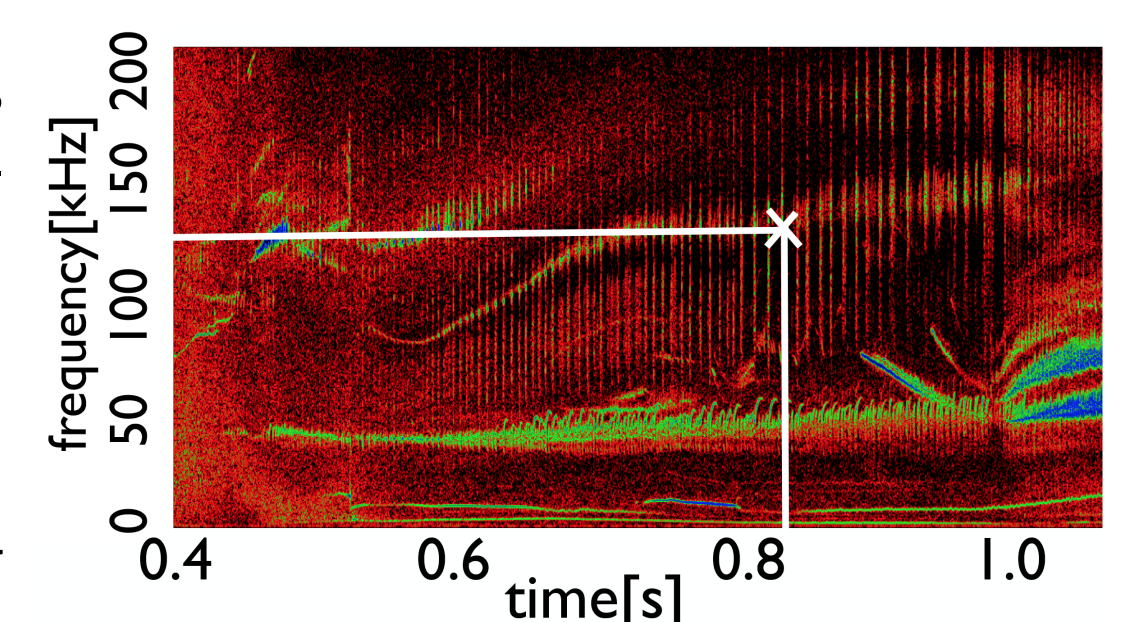


Figure 5

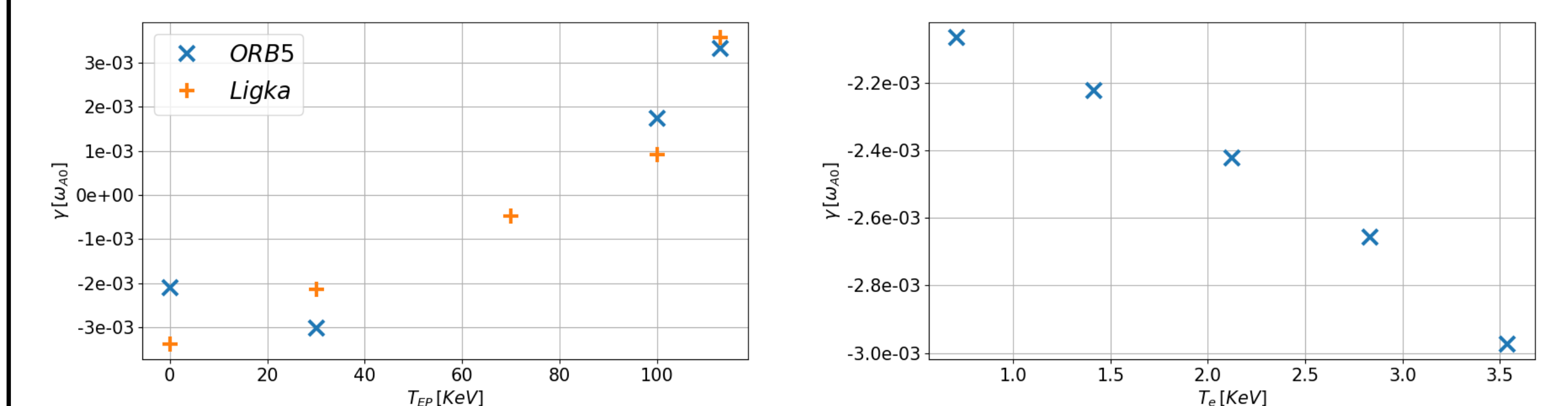
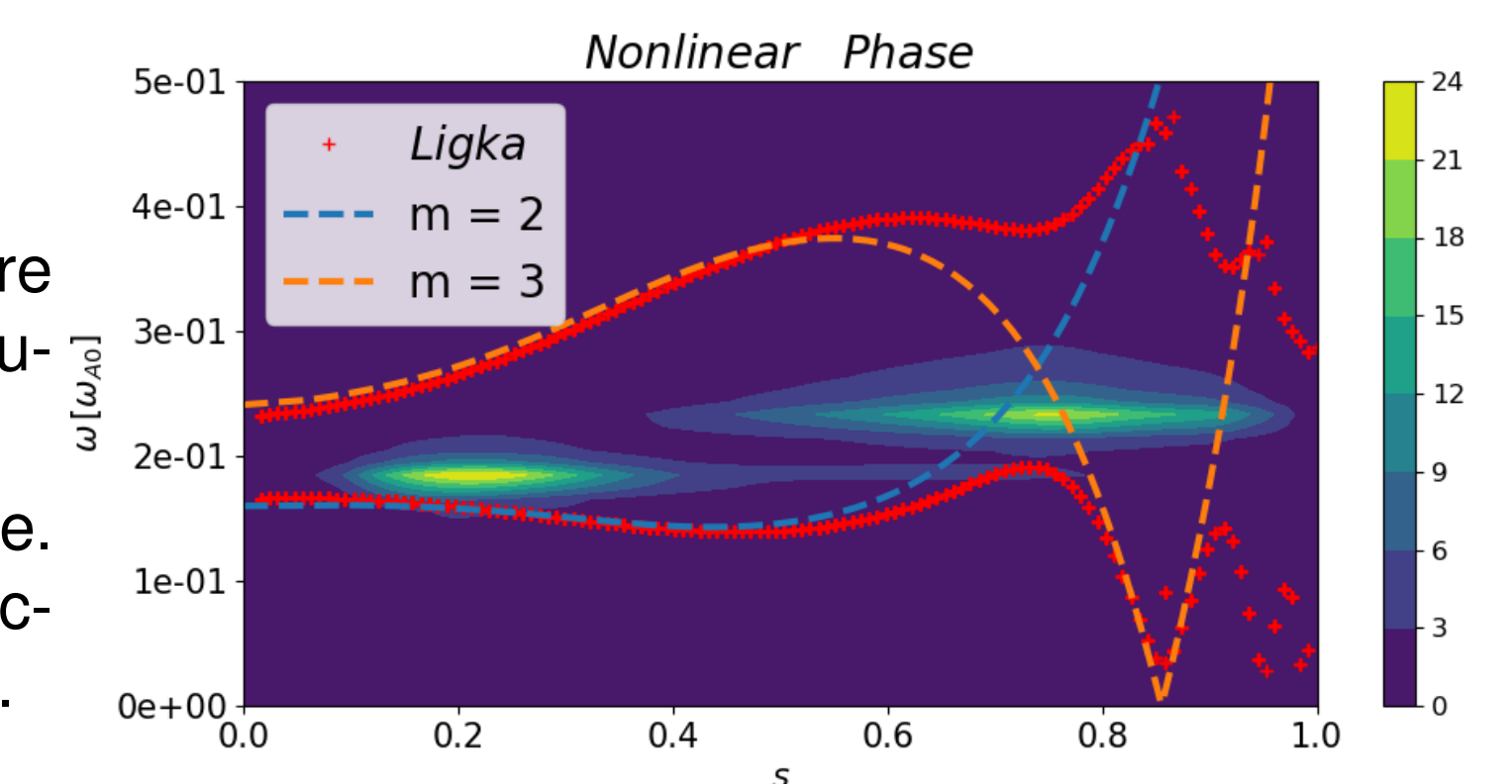


Figure 6: **Left:** Scan in the energetic particle temperature (T_{EP}). TAE growth rate calculated with LIGKA and ORB5 for a fraction of EP equal to 3% (same density, temperature profiles in use). **Right:** Landau damping dependence against the electron temperature.

4.2 NLED-AUG case: nonlinear results

- Nonlinear simulations are in progress.
- Preliminary results with off-axis EP profiles are displayed, with the frequency spectra calculated in the nonlinear phase.
- Nonlinear modification of the frequency (i.e. chirping) and the coexistence of energetic-particle continuum modes (EPMs) and TAEs.



5. Conclusions and Outlook

- Continuum damping and electron Landau damping investigated with ORB5 in simplified equilibria.
- Alfvén modes in **ASDEX Upgrade** investigated for the first time with **ORB5**, using experimental magnetic equilibrium and experimental profiles.
- Electron Landau damping found to be dominant, determining the linear growth rates and the nonlinear saturation.
- Comparisons with HYMAGYC [14] are in progress.
- **Next step 1:** More realistic distribution functions to be used.
- **Next step 2:** Nonlinear dynamics with Alfvén eigenmodes and EGAMs [15].